Received September 9, 2020, accepted September 27, 2020, date of publication October 2, 2020, date of current version October 20, 2020.

Digital Object Identifier 10.1109/ACCESS.2020.3028450

Constant Reflection Attenuation Constraint for Incoming Signals on Metasurface in Positional Modulation Design

BIN LIANG, JUN SHI, AND BO ZHANG, (Member, IEEE)

Tianjin Key Laboratory of Wireless Mobile Communications and Power Transmission, College of Electronic and Communication Engineering, Tianjin Normal University, Tianjin 300387, China

Corresponding author: Bin Liang (wdxylb@tjnu.edu.cn)

This work was supported in part by the Applied Development Research Fund of Tianjin Normal University under Grant 52XK1409, in part by the Doctor Fund of Tianjin Normal University under Grant 52XB2006, and in part by the Science and Technology Development Fund of Tianjin Education Commission for Higher Education under Grant 2019KJ087.

ABSTRACT Metasurface based positional modulation design has been introduced recently, where a given modulation pattern can only be received at certain desired positions by the proposed method. However, the magnitude of weight coefficient of each element on metasurface varies from one other, representing an attenuation of the amplitude of incoming signal in different degrees. In this paper, a constant reflection attenuation constraint for incoming signals is proposed for the first time, and the proposed method can be extended with a post-processing process to the ideal case where there is no reflection attenuation.

INDEX TERMS Positional modulation, metasurface, constant reflection attenuation constraint.

I. INTRODUCTION

With the rapid development of wireless network technology, the role of information security becomes more important than ever. In recent years, physical layer security technology has attracted great attention. As one of the technologies, directional modulation (DM) has been studied widely [1]–[18]. However, one of the DM problem is that when eavesdroppers are in the same direction as the desired receiver, their modulation patterns are similar. Then, with a high sensitivity receiver, the private signals transmitted only for the desired receiver can be cracked by eavesdroppers. To solve the problem, DM is extended to positional modulation (PM) where a given modulation pattern can only be received at certain desired positions. In [19], [20], frequency diverse antenna arrays have been used to achieve PM due to its consideration of distance between the transmitter to receivers. For phased antenna array designs, PM can be achieved by exploiting multi-path effect of signals. In [21], a reflecting surface was proposed, followed by multiple antenna arrays design in [22].

Recently, to further increase the degree of freedom in PM design, metasurface has been introduced as a replacement of reflecting surface [23]. As a newly proposed material, metasurface has been applied quickly in wireless communications [24]–[28]. However, to our best knowledge, the magnitude of each element on metasurface varies from one another, representing an attenuation of the amplitude of incoming signal in different degrees. In this paper, a constant reflection attenuation constraint for incoming signals is proposed for the first time, and the proposed method can be extended with a post-processing process to the ideal case where there is no reflection attenuation.

The remaining part of this paper is structured as follows. A review of metasurface based PM design is given in Sec. II. A constant reflection attenuation constraint for incoming signals on metasurface for PM design is presented in Sec. III. Design examples are provided in Sec. IV, followed by conclusions in Sec. V.

II. REVIEW OF METASURFACE BASED PM DESIGN

A Q-element metasurface with an N-element linear antenna array employed for positional modulation design is shown in Fig. 1. The vertical distance between the metasurface and the transmitting array is represented by H. Weight coefficient for the n-th antenna is represented by w_n ($n = 0, 1, \ldots, N-1$), and coefficient for the q-th unit on the metasurface is represented by $\tilde{w}_q$ ($q = 0, 1, \ldots, Q-1$). The distance between antennas is denoted by d_n, and the distance

The associate editor coordinating the review of this manuscript and approving it for publication was Qilian Liang.

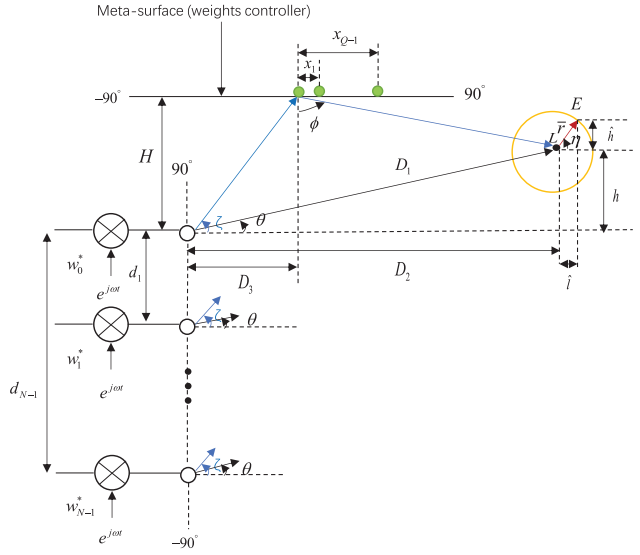

FIGURE 1. Metasurface based positional modulation design.

between units on the metasurface is denoted by x_q. L and E represent the desired receiver and eavesdropper, respectively. In the two-ray model, θ represents the direct angle from the transmitter to the receiver with the distance D_1, while ζ and ϕ represent the direct angle from the transmitter to the metasurface, and the direct angle from metasurface to the receiver, respectively. The steering vectors for the three direct paths are functions of θ, ζ and ϕ, respectively, given by

$$\begin{aligned}\mathbf{s}(\omega,\theta) &= [1, e^{j\omega d_1 \sin\theta/c}, \ldots, e^{j\omega d_{N-1}\sin\theta/c}]^T,\\ \hat{\mathbf{s}}(\omega,\zeta) &= [1, e^{j\omega d_1 \sin\zeta/c}, \ldots, e^{j\omega d_{N-1}\sin\zeta/c}]^T,\\ \tilde{\mathbf{s}}(\omega,\phi) &= [1, e^{-j\omega x_1 \sin\phi/c}, \ldots, e^{-j\omega x_{Q-1}\sin\phi/c}]^T. \end{aligned} \quad (1)$$

The weight vector for the transmitting array can be represented by

$$\mathbf{w} = [w_0, w_1, \ldots, w_{N-1}]^T, \quad (2)$$

and the counterpart for the metasurface is

$$\tilde{\mathbf{w}} = [\tilde{w}_0, \tilde{w}_1, \ldots, \tilde{w}_{Q-1}]. \quad (3)$$

Then, the beam response is

$$p(\theta,\zeta,\phi) = \mathbf{w}^H\mathbf{s}(\omega,\theta) + (\mathbf{w}^H\hat{\mathbf{s}}(\omega,\zeta)\cdot\tilde{\mathbf{w}})\tilde{\mathbf{s}}(\omega,\phi), \quad (4)$$

where $\cdot$ represents element-wise multiplication.

To have M symbols in the modulation pattern for PM design, the following vector is constructed, representing weight coefficients of the antenna array for the m-th symbol

$$\mathbf{w}_m = [w_{m,0}, \ldots, w_{m,N-1}]^T, \quad m = 0, \ldots, M-1. \quad (5)$$

Moreover, without loss of generality, assume r desired locations and $R-r$ eavesdropper locations in the design; then, based on these locations, we have the corresponding transmission angles θ_k, ζ_k and ϕ_k for $k = 0, \ldots, r-1, r, \ldots, R-1$, with steering matrices $\mathbf{S}_L, \mathbf{S}_E, \hat{\mathbf{S}}, \tilde{\mathbf{S}}_L$ and $\tilde{\mathbf{S}}_E$. Similarly, we can classify beam responses for desired locations $\mathbf{p}_{m,L}$ and beam responses for eavesdroppers $\mathbf{p}_{m,E}$, respectively [23].

To keep one set of $\tilde{\mathbf{w}}$ available for all M symbols, the following matrices are formulated

$$\begin{aligned}\mathbf{P}_E &= [\mathbf{p}_{0,E}; \mathbf{p}_{1,E}; \ldots; \mathbf{p}_{M-1,E}],\\ \mathbf{P}_L &= [\mathbf{p}_{0,L}; \mathbf{p}_{1,L}; \ldots; \mathbf{p}_{M-1,L}],\\ \mathbf{W} &= [\mathbf{w}_0, \mathbf{w}_1, \ldots, \mathbf{w}_{M-1}],\\ \mathbf{Y} &= \mathbf{P}_E - (\mathbf{W}^H\mathbf{S}_E + \mathbf{W}^H\hat{\mathbf{S}}_E\tilde{\mathbf{W}}\tilde{\mathbf{S}}_E), \end{aligned} \quad (6)$$

where $\tilde{\mathbf{W}} = diag(\tilde{\mathbf{w}})$ and $diag$ represents vector diagonalization.

Note that the metasurface has no amplifying function, then

$$||\tilde{\mathbf{w}}||_\infty \le 1. \quad (7)$$

Therefore, the corresponding PM design can be given by

$$\begin{aligned}&\min_{\mathbf{W},\tilde{\mathbf{w}}} ||[\mathbf{Y}(1,:), \mathbf{Y}(2,:), \ldots, \mathbf{Y}(M,:)]||_2\\ &\text{subject to } \mathbf{W}^H\mathbf{S}_L + \mathbf{W}^H\hat{\mathbf{S}}_L\tilde{\mathbf{W}}\tilde{\mathbf{S}}_L = \mathbf{P}_L\\ &\qquad ||\tilde{\mathbf{w}}||_\infty \le 1. \end{aligned} \quad (8)$$

III. CONSTANT REFLECTION ATTENUATION CONSTRAINT FOR INCOMING SIGNALS ON THE METASURFACE

Based on formulation (8), magnitude of the q-th weight coefficient on the metasurface can be any value but no larger than 1 ($q = 0, 1, \ldots, Q-1$), representing an attenuation of the amplitude of the incoming signal on each element of the metasurface in different degrees. Therefore, in this section, we introduce a constraint below to keep a constant attenuation for incoming signals on the metasurface, and it can be extended to the ideal case where there is no reflection attenuation

$$|\tilde{w}_0| = |\tilde{w}_1| = \ldots = |\tilde{w}_{Q-1}|. \quad (9)$$

Then, the PM design with the constant reflection attenuation constraint is given by

$$\begin{aligned}&\min_{\mathbf{W},\tilde{\mathbf{w}}} ||[\mathbf{Y}(1,:), \mathbf{Y}(2,:), \ldots, \mathbf{Y}(M,:)]||_2\\ &\text{subject to } \mathbf{W}^H\mathbf{S}_L + \mathbf{W}^H\hat{\mathbf{S}}_L\tilde{\mathbf{W}}\tilde{\mathbf{S}}_L = \mathbf{P}_L\\ &\qquad ||\tilde{\mathbf{w}}||_\infty \le 1\\ &\qquad |\tilde{w}_0| = |\tilde{w}_1| = \ldots = |\tilde{w}_{Q-1}|. \end{aligned} \quad (10)$$

However, due to the equality constraint (9), formulation (10) is non-convex, resulting in an un-solvable problem by existing optimisation tools. Therefore, in the work, we borrow the MinMax method to keep the same magnitude value for all symbols [29]. Then, constraint (9) can be replaced by

$$\begin{aligned}|\tilde{w}_0| &= |\tilde{w}_1| = \ldots = |\tilde{w}_{Q-1}|\\ &\rightarrow \min(\max([|\tilde{w}_0|, |\tilde{w}_1|, \ldots, |\tilde{w}_{Q-1}|]))\\ &\rightarrow \min||\tilde{\mathbf{w}}||_\infty, \end{aligned} \quad (11)$$

where $||\cdot||_\infty$ represents l_∞ norm. Based on it, formulation (10) can be changed to

$$\min_{\mathbf{W},\tilde{\mathbf{w}}} ||[\mathbf{Y}(1,:), \mathbf{Y}(2,:), \ldots, \mathbf{Y}(M,:)]||_2$$

$$\begin{aligned} &\text{subject to } \mathbf{W}^H\mathbf{S}_L + \mathbf{W}^H\hat{\mathbf{S}}_L\tilde{\mathbf{W}}\tilde{\mathbf{S}}_L = \mathbf{P}_L \\ &\quad ||\tilde{\mathbf{w}}||_\infty \le 1 \\ &\quad \min ||\tilde{\mathbf{w}}||_\infty. \end{aligned} \tag{12}$$

To our best knowledge, in previous PM designs the formulation has either multiple sets of variables or multiple objective functions, but none of the PM designs consider both scenarios. For the above formulation (12), multiple sets of variables $\mathbf{W}$ and $\tilde{\mathbf{w}}$, multiple objective functions $\min||[\mathbf{Y}(1,:), \mathbf{Y}(2,:), \ldots, \mathbf{Y}(M,:)]||_2$ and $\min ||\tilde{\mathbf{w}}||_\infty$ are included in the design. Here, we consider a two-phase method to solve the problem, and it is available for all frequencies.

Phase 1: we solve the problem of multiple cost functions. We introduce a parameter μ where μ is a trade-off factor ranging from 0 to 1 to combine multiple cost functions into one. Based on it, the cost function in (12) becomes

$$\min_{\mathbf{W},\tilde{\mathbf{w}}} \mu||[\mathbf{Y}(1,:), \mathbf{Y}(2,:), \ldots, \mathbf{Y}(M,:)]||_2 + (1-\mu)||\tilde{\mathbf{w}}||_\infty. \tag{13}$$

Then, formulation (12) can be written as

$$\begin{aligned} &\min_{\mathbf{W},\tilde{\mathbf{w}}} \mu||[\mathbf{Y}(1,:), \mathbf{Y}(2,:), \ldots, \mathbf{Y}(M,:)]||_2 + (1-\mu)||\tilde{\mathbf{w}}||_\infty \\ &\text{subject to } \mathbf{W}^H\mathbf{S}_L + \mathbf{W}^H\hat{\mathbf{S}}_L\tilde{\mathbf{W}}\tilde{\mathbf{S}}_L = \mathbf{P}_L \\ &\quad ||\tilde{\mathbf{w}}||_\infty \le 1. \end{aligned} \tag{14}$$

Phase 2: we solve the problem of multiple sets of variables. Similar to [23], an alternating optimization method can be adapted, with the process below

1) Randomly generate the vector $\tilde{\mathbf{w}}$ with all magnitudes the same as a given value.
2) With the provided $\tilde{\mathbf{w}}$, $\mathbf{W}$ in (14) can be optimised.
3) Set $\mathbf{W}$ as a given value, $\tilde{\mathbf{w}}$ in (14) can be optimised.
4) Repeat 2) and 3) until the cost function in (14) converges.

The above problem (14) can be solved by the CVX toolbox in MATLAB [30], [31].

Note that all magnitudes of weight coefficients of the metasurface calculated by the above alternating optimization method cannot be set as a pre-defined value σ. Therefore, we introduce a post-processing process. By keeping the phase while increasing or decreasing the magnitude uniformly, the weight coefficients can be satisfied for all required attenuations. The process is given below:

1) Set the parameter ρ equals to the angle of $\tilde{\mathbf{w}}$ ($\rho = \angle\tilde{\mathbf{w}}$).
2) Set $\tilde{\mathbf{w}}$ as the new value with the pre-defined magnitude σ no larger than 1 and phase shift ρ ($\tilde{\mathbf{w}} = \sigma e^{j\rho}$).

IV. DESIGN EXAMPLES

A 64-unit metasurface and a 50-element linear antenna array are constructed for positional modulation design, with a distance between adjacent elements $x = n = \lambda/2$. One desired receiver is located at $\theta = 0°$, with $H = 1000\lambda$ and $D_1 = 900\lambda$. Eavesdroppers are located around the desired receiver with $\bar{r} = \lambda$ and $\eta \in [0°, 360°)$, sampled every 10°. The desired response at the desired location obeys the QPSK modulation mode, while the magnitude is down to 0.2 at eavesdropper locations with a random phase shift. The signal to noise ratio is set at 12 dB at the desired location, with the same level of noise at other locations. $\mu = 0.2$ is selected for the trade-off factor by trial and error. Moreover, all reflection

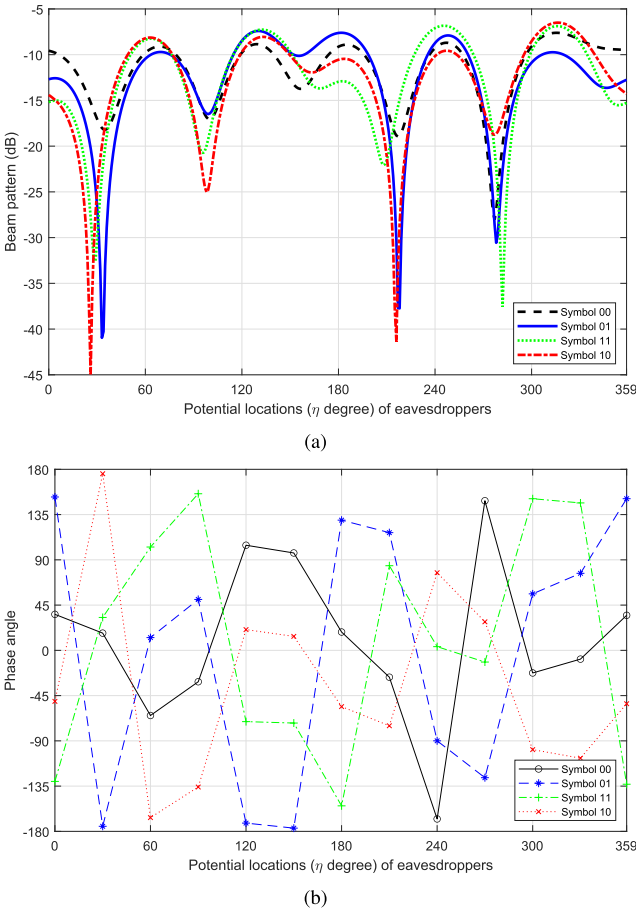

FIGURE 2. Resultant beam and phase patterns for eavesdroppers without reflection attenuation constraint in (8).

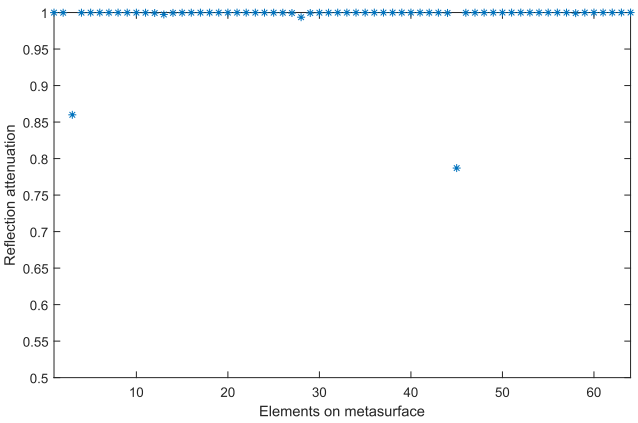

FIGURE 3. Reflection attenuation of elements on metasurface without reflection attenuation constraint in (8).

TABLE 1. Weight coefficients on metasurface in (8).

q	$\tilde{w}_q$	q	$\tilde{w}_q$	q	$\tilde{w}_q$	q	$\tilde{w}_q$
1	$0.6773-0.7356i$	17	$-0.1668+0.9858i$	33	$0.4342+0.9007i$	49	$0.9004+0.4348i$
2	$0.1153-0.9930i$	18	$0.4598+0.8879i$	34	$0.8843+0.4666i$	50	$0.9839-0.1781i$
3	$0.2682+0.8170i$	19	$0.8989+0.4379i$	35	$0.9886-0.1499i$	51	$0.6906-0.7231i$
4	$0.9107+0.4125i$	20	$0.9829-0.1835i$	36	$0.7068-0.7072i$	52	$0.1331-0.9910i$
5	$0.9782-0.2070i$	21	$0.6791-0.7339i$	37	$0.1500-0.9886i$	53	$-0.4730-0.8810i$
6	$0.6655-0.7462i$	22	$0.1078-0.9940i$	38	$-0.4656-0.8849i$	54	$-0.8988-0.4381i$
7	$0.0924-0.9956i$	23	$-0.5082-0.8610i$	39	$-0.8982-0.4394i$	55	$-0.9861+0.1656i$
8	$-0.5186-0.8549i$	24	$-0.9244-0.3810i$	40	$-0.9838+0.1786i$	56	$-0.7134+0.7006i$
9	$-0.9270-0.3747i$	25	$-0.9647+0.2623i$	41	$-0.6893+0.7243i$	57	$-0.2194+0.9755i$
10	$-0.9643+0.2642i$	26	$-0.5921+0.8055i$	42	$-0.1286+0.9915i$	58	$-0.7314+0.6808i$
11	$-0.5873+0.8090i$	27	$0.1391+0.9896i$	43	$0.4892+0.8719i$	59	$-0.9581-0.2859i$
12	$0.1249+0.9915i$	28	$0.8792-0.4629i$	44	$0.9145+0.4032i$	60	$-0.9618+0.2736i$
13	$0.7385-0.6703i$	29	$-0.7476-0.6632i$	45	$-0.6927-0.3735i$	61	$-0.6325+0.7746i$
14	$-0.7964-0.6040i$	30	$-0.9984+0.0523i$	46	$-0.7167+0.6969i$	62	$-0.0651+0.9979i$
15	$-0.9959+0.0877i$	31	$-0.7511+0.6598i$	47	$-0.1435+0.9895i$	63	$0.5300+0.8480i$
16	$-0.7295+0.6837i$	32	$-0.1969+0.9803i$	48	$0.4702+0.8824i$	64	$0.9262+0.3770i$

TABLE 2. Weight coefficients on metasurface in (14).

q	$\tilde{w}_q$	q	$\tilde{w}_q$	q	$\tilde{w}_q$	q	$\tilde{w}_q$
1	$0.3549-0.3475i$	17	$-0.4715-0.1563i$	33	$0.4967-0.0083i$	49	$0.4892+0.0859i$
2	$0.1053-0.4854i$	18	$-0.4823+0.1189i$	34	$0.3912-0.3061i$	50	$0.4289-0.2507i$
3	$-0.1752-0.4648i$	19	$-0.3407+0.3615i$	35	$0.1245-0.4809i$	51	$0.1739-0.4653i$
4	$-0.3966-0.2991i$	20	$-0.0855+0.4893i$	36	$-0.1971-0.4560i$	52	$-0.1524-0.4728i$
5	$-0.4946-0.0465i$	21	$0.2015+0.4540i$	37	$-0.4380-0.2344i$	53	$-0.4091-0.2818i$
6	$-0.4484+0.2137i$	22	$0.4220+0.2620i$	38	$-0.4874+0.0957i$	54	$-0.4964+0.0182i$
7	$-0.2820+0.4089i$	23	$0.4962-0.0236i$	39	$-0.3093+0.3887i$	55	$-0.3955+0.3006i$
8	$-0.0488+0.4943i$	24	$0.3937-0.3029i$	40	$0.0301+0.4958i$	56	$-0.1796+0.4631i$
9	$0.1893+0.4592i$	25	$0.1480-0.4742i$	41	$0.3681+0.3335i$	57	$-0.0321+0.4957i$
10	$0.3790+0.3211i$	26	$-0.1535-0.4724i$	42	$0.4944-0.0477i$	58	$-0.3431+0.3592i$
11	$0.4834+0.1142i$	27	$-0.3994-0.2953i$	43	$0.2686-0.4178i$	59	$-0.3449+0.3575i$
12	$0.4823-0.1188i$	28	$-0.4967-0.0065i$	44	$-0.1864-0.4605i$	60	$-0.1318+0.4789i$
13	$0.3718-0.3294i$	29	$-0.4060+0.2862i$	45	$-0.4828-0.1167i$	61	$0.1620+0.4696i$
14	$0.1690-0.4671i$	30	$-0.1593+0.4705i$	46	$-0.3948+0.3015i$	62	$0.4098+0.2808i$
15	$-0.0836-0.4897i$	31	$0.1504+0.4734i$	47	$-0.0487+0.4943i$	63	$0.4959-0.0283i$
16	$-0.3208-0.3792i$	32	$0.4027+0.2908i$	48	$0.3078+0.3899i$	64	$0.3705-0.3309i$

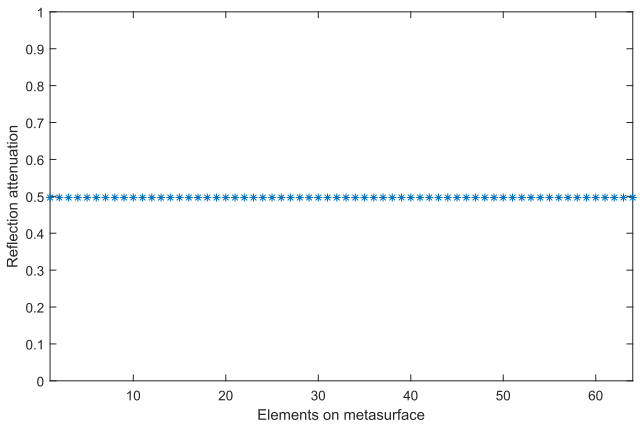

FIGURE 4. Reflection attenuation of elements on metasurface with the constant reflection attenuation constraint in (14).

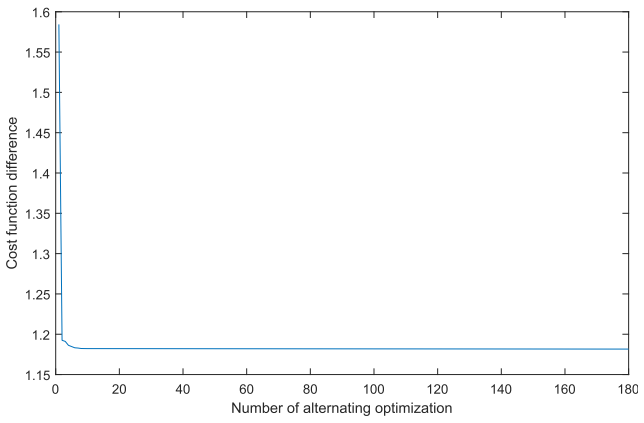

FIGURE 5. Cost function difference in (14).

attenuation of units on the metasurface are required to be the same, and there is no attenuation reflection for the ideal case ($\sigma = 1$).

The resultant beam and phase patterns for the eavesdroppers based on the PM design without the constant reflection attenuation constraint for incoming singals on the metasurface in (8) are shown in Figs. 2(a) and 2(b), where beam response level at all eavesdropper locations are lower than -5dB, and the phase of signal at these locations are random. However, as shown in Fig. 3, the reflection attenuation for all elements on metasurface are not the same, i.e. the reflection attenuation is 0.8599 for the 3-rd element, 0.9936 for the 28-th element, 0.787 for the 45-th element, and 0.9999 for the rest of the elements, demonstrating the

TABLE 3. Weight coefficients on metasurface after post processing.

q	$\tilde{w}_q$	q	$\tilde{w}_q$	q	$\tilde{w}_q$	q	$\tilde{w}_q$
1	$0.7145-0.6996i$	17	$-0.9492-0.3147i$	33	$0.9999-0.0167i$	49	$0.9849+0.1730i$
2	$0.2120-0.9773i$	18	$-0.9709+0.2394i$	34	$0.7875-0.6163i$	50	$0.8633-0.5046i$
3	$-0.3527-0.9357i$	19	$-0.6858+0.7277i$	35	$0.2506-0.9681i$	51	$0.3501-0.9367i$
4	$-0.7985-0.6020i$	20	$-0.1721+0.9851i$	36	$-0.3968-0.9179i$	52	$-0.3067-0.9518i$
5	$-0.9956-0.0936i$	21	$0.4057+0.9140i$	37	$-0.8817-0.4718i$	53	$-0.8235-0.5673i$
6	$-0.9028+0.4301i$	22	$0.8496+0.5275i$	38	$-0.9812+0.1928i$	54	$-0.9993+0.0365i$
7	$-0.5677+0.8232i$	23	$0.9989-0.0476i$	39	$-0.6226+0.7825i$	55	$-0.7961+0.6052i$
8	$-0.0982+0.9952i$	24	$0.7926-0.6098i$	40	$0.0607+0.9982i$	56	$-0.3615+0.9324i$
9	$0.3811+0.9245i$	25	$0.2979-0.9546i$	41	$0.7411+0.6714i$	57	$-0.0647+0.9979i$
10	$0.7629+0.6465i$	26	$-0.3089-0.9511i$	42	$0.9954-0.0961i$	58	$-0.6907+0.7231i$
11	$0.9732+0.2299i$	27	$-0.8041-0.5945i$	43	$0.5408-0.8411i$	59	$-0.6943+0.7197i$
12	$0.9710-0.2391i$	28	$-0.9999-0.0130i$	44	$-0.3752-0.9270i$	60	$-0.2654+0.9641i$
13	$0.7485-0.6631i$	29	$-0.8174+0.5761i$	45	$-0.9720-0.2349i$	61	$0.3262+0.9453i$
14	$0.3401-0.9404i$	30	$-0.3207+0.9472i$	46	$-0.7947+0.6070i$	62	$0.8249+0.5653i$
15	$-0.1682-0.9857i$	31	$0.3027+0.9531i$	47	$-0.0980+0.9952i$	63	$0.9984-0.0569i$
16	$-0.6458-0.7635i$	32	$0.8107+0.5855i$	48	$0.6196+0.7849i$	64	$0.7458-0.6661i$

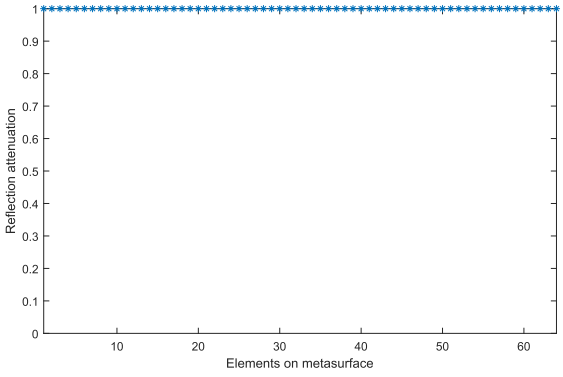

FIGURE 6. Reflection attenuation of elements on metasurface with the constant reflection attenuation constraint after post processing.

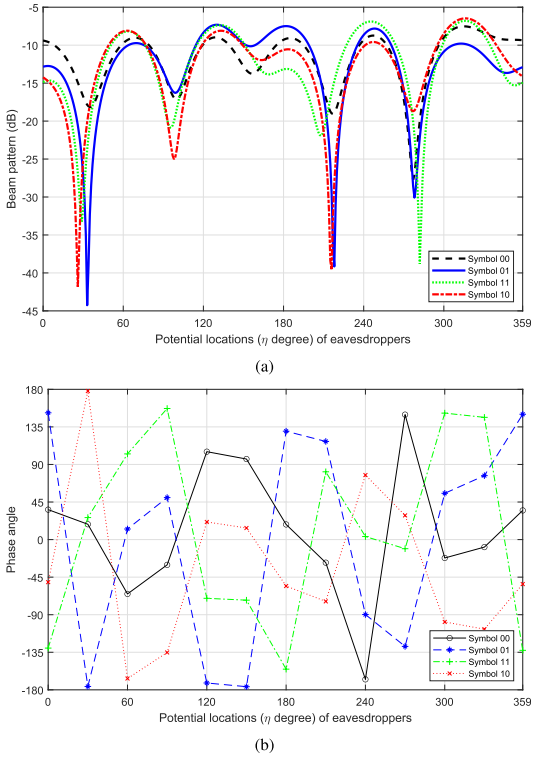

FIGURE 7. Resultant beam and phase patterns for eavesdroppers with the constant reflection attenuation after post processing.

un-satisfactory of the design requirement. The corresponding weight coefficients are shown in Table 1.

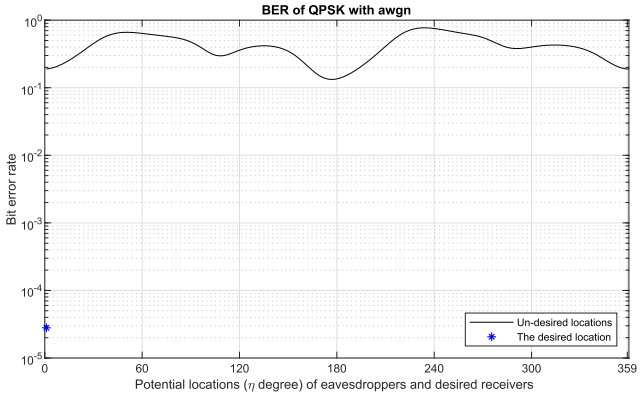

FIGURE 8. BERs patterns for the eavesdroppers and desired receiver with the constant reflection attenuation constraint after post processing.

For the PM design with the constant reflection attenuation constraint in (14), reflection attenuation for all elements on metasurface are shown in Fig. 4. Here we can see the same reflection attenuation 0.4967 are achieved for all elements, with the corresponding weight coefficients shown in Table 2, demonstrating the effectiveness of the proposed design. Fig. 5 shows the corresponding cost function difference in (14), representing the achievement of the cost function convergence.

For the requirement of no reflection attenuation in the ideal scenario ($\sigma = 1$), $\tilde{\mathbf{w}}$ calculated by (14) is post-processed, where the angle of $\tilde{\mathbf{w}}$ is kept with the magnitude set at $\sigma = 1$, as shown in Fig. 6. Then, with the new $\tilde{\mathbf{w}}$ shown in Table 3, the beam pattern and phase pattern are shown in Figs. 7(a) and 7(b). Fig 8 shows the bit error rate (BER) of the proposed design, where the BER of the desired location is the lowest and down to 10^{-5}, but it is fluctuated at un-desired locations, demonstrating the achievement of the PM design.

V. CONCLUSION

In this paper, a constant reflection attenuation constraint for incoming signals on the metasurface is proposed for the first time, and the proposed method can be extended to the ideal case with a post-processing process where there is no reflection attenuation. As shown in the given figures, with the proposed constraint, reflection attenuation of all elements on the metasurface can be constrained to a pre-defined value, with a satisfactory of the PM design.

REFERENCES

[1] A. Babakhani, D. B. Rutledge, and A. Hajimiri, "Near-field direct antenna modulation," *IEEE Microw. Mag.*, vol. 10, no. 1, pp. 36–46, Feb. 2009.

[2] M. P. Daly and J. T. Bernhard, "Directional modulation technique for phased arrays," *IEEE Trans. Antennas Propag.*, vol. 57, no. 9, pp. 2633–2640, Sep. 2009.

[3] M. P. Daly and J. T. Bernhard, "Beamsteering in pattern reconfigurable arrays using directional modulation," *IEEE Trans. Antennas Propag.*, vol. 58, no. 7, pp. 2259–2265, Jul. 2010.

[4] T. Hong, M.-Z. Song, and Y. Liu, "Dual-beam directional modulation technique for physical-layer secure communication," *IEEE Antennas Wireless Propag. Lett.*, vol. 10, pp. 1417–1420, Dec. 2011.

[5] Q. Zhu, S. Yang, R. Yao, and Z. Nie, "Directional modulation based on 4-D antenna arrays," *IEEE Trans. Antennas Propag.*, vol. 62, no. 2, pp. 621–628, Feb. 2014.

[6] Y. Ding and V. F. Fusco, "A vector approach for the analysis and synthesis of directional modulation transmitters," *IEEE Trans. Antennas Propag.*, vol. 62, no. 1, pp. 361–370, Jan. 2014.

[7] Y. He, Y. Liu, N. Du, and N. Xie, "Directional modulation for QAM signals with PAPR reduction," in *Proc. 46th Eur. Microw. Conf. (EuMC)*, Oct. 2016, pp. 1307–1310.

[8] J. Hu, F. Shu, and J. Li, "Robust synthesis method for secure directional modulation with imperfect direction angle," *IEEE Commun. Lett.*, vol. 20, no. 6, pp. 1084–1087, Jun. 2016.

[9] H. Shi and A. Tennant, "Enhancing the security of communication via directly modulated antenna arrays," *IET Microw., Antennas Propag.*, vol. 7, no. 8, pp. 606–611, Jun. 2013.

[10] Y. Ding and V. Fusco, "Directional modulation transmitter radiation pattern considerations," *IET Microw., Antennas Propag.*, vol. 7, no. 15, pp. 1201–1206, Dec. 2013.

[11] B. Guo, Y.-H. Yang, G. Xin, and Y.-Q. Tang, "Combinatorial interference directional modulation for physical layer security transmission," in *Proc. IEEE Inf. Technol., Netw., Electron. Autom. Control Conf.*, May 2016, pp. 710–713.

[12] A. Kalantari, M. Soltanalian, S. Maleki, S. Chatzinotas, and B. Ottersten, "Directional modulation via symbol-level precoding: A way to enhance security," *IEEE J. Sel. Topics Signal Process.*, vol. 10, no. 8, pp. 1478–1493, Dec. 2016.

[13] S. Mufti, A. Tennant, and J. Parrón, "Dual channel broadcast using phase-only directional modulation system," in *Proc. IEEE Int. Symp. Antennas Propag. USNC/URSI Nat. Radio Sci. Meeting*, Jul. 2018, pp. 2219–2220.

[14] B. Zhang, W. Liu, and X. Lan, "Orthogonally polarized dual-channel directional modulation based on crossed-dipole arrays," *IEEE Access*, vol. 7, pp. 34198–34206, 2019.

[15] N. Valliappan, A. Lozano, and R. W. Heath, Jr., "Antenna subset modulation for secure millimeter-wave wireless communication," *IEEE Trans. Commun.*, vol. 61, no. 8, pp. 3231–3245, Aug. 2013.

[16] Y. Ding and V. F. Fusco, "Directional modulation far-field pattern separation synthesis approach," *IET Microw., Antennas Propag.*, vol. 9, no. 1, pp. 41–48, Jan. 2015.

[17] T. Xie, J. Zhu, and Y. Li, "Artificial-noise-aided zero-forcing synthesis approach for secure multi-beam directional modulation," *IEEE Commun. Lett.*, vol. 22, no. 2, pp. 276–279, Feb. 2018.

[18] B. Zhang, W. Liu, Y. Li, X. Zhao, and C. Wang, "Directional modulation design under a constant magnitude constraint for weight coefficients," *IEEE Access*, vol. 7, pp. 154711–154718, 2019.

[19] Y. Ding, V. Fusco, and J. Zhang, "Frequency diverse array OFDM transmitter for secure wireless communication," *Electron. Lett.*, vol. 51, no. 17, pp. 1374–1376, Aug. 2015.

[20] J. Hu, S. Yan, F. Shu, J. Wang, J. Li, and Y. Zhang, "Artificial-noise-aided secure transmission with directional modulation based on random frequency diverse arrays," *IEEE Access*, vol. 5, pp. 1658–1667, 2017.

[21] H. Shi and A. Tennant, "Secure communications based on directly modulated antenna arrays combined with multi-path," in *Proc. Loughborough Antennas Propag. Conf. (LAPC)*, Loughborough, U.K., Nov. 2013, pp. 582–586.

[22] B. Zhang and W. Liu, "Positional modulation design based on multiple phased antenna arrays," *IEEE Access*, vol. 7, pp. 33898–33905, 2019.

[23] B. Zhang, W. Liu, Q. Li, Y. Li, X. Zhao, C. Zhang, and C. Wang, "Metasurface based positional modulation design," *IEEE Access*, vol. 8, pp. 113807–113813, 2020.

[24] L. B. Wang, K. Y. See, J. W. Zhang, B. Salam, and A. C. W. Lu, "Ultra-thin and flexible screen-printed metasurfaces for EMI shielding applications," *IEEE Trans. Electromagn. Compat.*, vol. 53, no. 3, pp. 700–705, Aug. 2011.

[25] S. V. Hum and J. Perruisseau-Carrier, "Reconfigurable reflectarrays and array lenses for dynamic antenna beam control: A review," *IEEE Trans. Antennas Propag.*, vol. 62, no. 1, pp. 183–198, Jan. 2014.

[26] C. Liaskos, S. Nie, A. Tsioliaridou, A. Pitsillides, S. Ioannidis, and I. Akyildiz, "A new wireless communication paradigm through software-controlled metasurfaces," *IEEE Commun. Mag.*, vol. 56, no. 9, pp. 162–169, Sep. 2018.

[27] Y. Liu, L. Zhang, B. Yang, W. Guo, and M. Imran, "Programmable wireless channel for multi-user MIMO transmission using meta-surface," in *Proc. IEEE Global Commun. Conf. (GLOBECOM)*, Waikoloa, HI, USA, Dec. 2019, pp. 1–6.

[28] L. Zhang, X. Q. Chen, S. Liu, Q. Zhang, J. Zhao, J. Y. Dai, G. D. Bai, X. Wan, Q. Cheng, G. Castaldi, V. Galdi, and T. J. Cui, "Space-Time-Coding Digital Metasurfaces," *Nature Commun.*, vol. 9, no. 1, p. 4334, Oct. 2018.

[29] B. Zhang, W. Liu, Y. Li, X. Zhao, C. Zhang, and C. Wang, "Symbol-independent weight magnitude design for antenna array based directional modulation," *Ad Hoc Netw.*, vol. 101, Apr. 2020, Art. no. 102097. [Online]. Available: http://www.sciencedirect.com/science/article/pii/S1570870519311217

[30] M. Grant and S. Boyd, "Graph implementations for nonsmooth convex programs," in *Recent Advances in Learning and Control* (Lecture Notes in Control and Information Sciences), V. Blondel, S. Boyd, and H. Kimura, Eds. London, U.K.: Springer-Verlag, 2008, pp. 95–110. [Online]. Available: http://stanford.edu/~boyd/graph_dcp.html

[31] CVX Research. (Sep. 2012). *CVX: MATLAB Software for Disciplined Convex Programming, Version 2.0 Beta*. [Online]. Available: http://cvxr.com/cvx

BIN LIANG received the B.Sc. degree from the Department of Automation, Tianjin University of Technology and Education, China, in 2004, and the M.Sc. degree from the College of Software, Nankai University, China, in 2016.

He is currently working with the College of Electronic and Communication Engineering, Tianjin Normal University. His research interests include embedded system design and application.

JUN SHI received the B.Sc. degree from Tianjin Normal University, China, in 2005, and the M.Sc. degree from the Department of Physics and Electronic Information, Tianjin Normal University, in 2008.

She is currently working with the College of Electronic and Communication Engineering, Tianjin Normal University. Her research interests include software and educational technology.

BO ZHANG (Member, IEEE) received the B.Sc. degree from Tianjin Normal University, China, in 2011, and the M.Sc. and Ph.D. degrees from the Department of Electrical and Electronic Engineering, The University of Sheffield, in 2013 and 2018, respectively.

He is currently working with the College of Electronic and Communication Engineering, Tianjin Normal University. His research interests include array signal processing (beamforming and direction of arrival estimation and so on), directional modulation, sparse array design, and natural language processing.